Supplementary information for Part 2

Justification of our method to confirm contact configuration between the detector and source--- examination with the use of ^{40}K in a KCl test source and in slabs of granite---

In this text the contact configuration means that the flat window of the pressure tight vessel (PTV) for incoming gamma rays touches a plane source or a plane specimen without a gap which is visible by the naked eye.

In Section 1, we prepare a flat test source of ^{40}K made of pure KCl powder, and flat slabs of granite as specimens of unknown activity of ^{40}K. It is shown that under the contact configuration between the detector and source, the observed count rate of the photopeak of ^{40}K is well reproduced by a simple model calculation for a test source of known activity of ^{40}K. A factor to convert the count rate of the photopeak of ^{40}K to the activity of ^{40}K in units of Bq underneath the detector is obtained.

In Section 2, it is shown that in the case of granite slabs of unknown concentration of ^{40}K, application of the conversion factor to observed count rates yields the concentration of ^{40}K in units of Bq/kg with an assumption of uniform distribution of ^{40}K in the slab. The result is in good agreement with the published data.

In Section 3, it is shown that the observed count rates of the photopeak of ^{40}K in the spectra reported in Part 1[1] are explained reasonably well with the use of the concentration of ^{40}K in the granite slabs. This fact leads to that the nearly uniform count rates over the measurement points indicate firmly that the contact configuration is established at every measurement point at the bottom of the sea. Therefore, the results of our measurements of ^{137}Cs on the surface of rock are thought to be credible.

1. ^{40}K test source
1. 1 Preparation of test source
A test source of ^{40}K is prepared from commercially available pure KCl powder (Hayashi Pure Chemical Ind., Ltd, Osaka, Japan. https://www.hpc-j.com/). The natural abundance of ^{40}K is 0.0117 %. The KCl powder of 500 g is packed in a square box. The volume of the box, V_{Box}, is 115 mm×115mm×30mm. The diameter of the cylindrical CsI(Tl) scintillator crystal and that of the window of the pressure tight vessel (PTV) for incoming gamma rays are 110 mm. Thus, the top surface of the KCl packed box is large enough to cover the window of the PTV. The bulk density of the KCl source is 1.26 g/cm^3.

1. 2 Activity of ^{40}K underneath the detector

For the sake of simplicity, we assume that in the contact configuration the detector sees only the underneath cylindrical part of the KCl source. The volume of the cylindrical part, V_{cyl}, is $\pi \times (55 \text{ mm})^2 \times 30$ mm. Then, the amount of KCl underneath the detector is, 500 (g)$\times V_{cyl} / V_{Box}$ =359.3 (g). Using the natural abundance of ^{40}K, the atomic weights of K and Cl, and the half-life of ^{40}K ($T_{1/2}$ =1.25$\times 10^9$ y), we get 5.81$\times 10^3$ Bq of ^{40}K in the KCl powder of 359.3 g, namely 1.62$\times 10^4$ Bq/kg.

1. 3 Measurements of energy spectra and count rate of the photopeak of ^{40}K

In order to measure the background spectrum, the detector in the PTV is placed on the floor of our laboratory with the window facing down. The materials of the concrete floor and walls of the laboratory inevitably contain ^{40}K. Thus, the background spectrum has the photopeak of ^{40}K and continuous spectrum in the region below the photopeak. The measurement of the background spectrum is made for 60 minutes. Then, the KCl test source is inserted between the floor and the PTV. The detector and the source are in the contact configuration. The spectrum of the test source is measured also for 60 minutes. When subtraction of the background from the spectrum of the KCl test source is carried out, attenuation of the background spectrum due to the thickness of the KCl test source is taken into account by the use of attenuation coefficient of KCl given by XCOM: Photon Cross Sections Data [2]. From the area under the photopeak of ^{40}K in the background-corrected spectrum we get 15.9 counts per second (cps) for the count rate of 1.46 MeV gamma rays. Figure 1S shows the background spectrum, and the spectrum of the test source with the background.
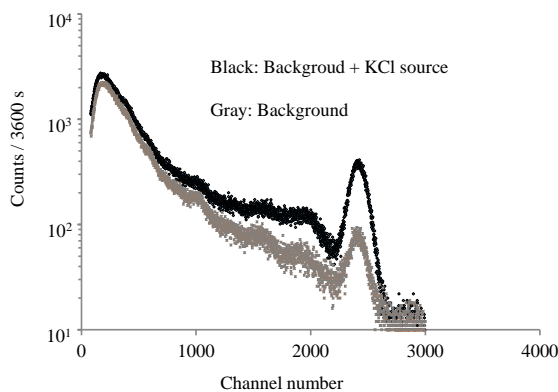

Fig. 1S Spectrum of background and that of KCl test source with background

1. 4 Estimation of the count rate based on a model calculation

An estimated count rate of the photopeak in the contact configuration between the

detector and the test source of 5.81×10^3 Bq of ^{40}K turns out to be 17.1 cps as calculated below.

Factors taken into consideration are;

    1. Ratio of 1.46 MeV gamma-ray decay: 0.107.

    2. Detection efficiency at 1.46 MeV: 0.42. (See Saint-Gobain Crystals [3].)

    3. Peak to Total ratio p: 0.2. (See Note 1 below and Saint-Gobain Crystals [3].)

    4. Ratio of the solid angle covered by the face of the detector to 4π: 0.369. (See Note 2 below.)

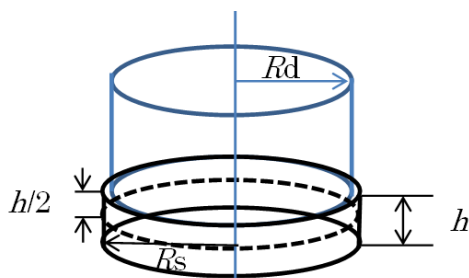   5. Effect of self-attenuation in the source: 0.911. (See Note 3 below.)

Multiplying the source activity of 5.81×10^3 (Bq) by these factors, we get 17.1 cps $\pm 10\%$.

Note 1: The peak to total ratio p

As described by Legg and Seaman [4], the peak to total ratio p is defined as the ratio between the number of counts in the full-energy peak and the total number of counts in the spectrum. The full-energy peak is the sum of the direct photoelectric absorption and all the processes of total deposition of energies of photons in the scintillator crystal, such as the Compton scattering with the secondary photon undergoing photoelectric absorption. Since the present situation of high background due to ^{40}K in the floor and the walls makes it difficult to empirically determine a reliable peak to total ratio, we use the results of Monte Carlo simulation given by Saint-Gobain Crystals [3].

Note 2: The solid angle subtended by the detector

Figure 2S below shows the contact configuration between the cylindrical detector and a cylindrical homogeneous source of height h. We calculate the height-averaged solid angle at a plane in the source at $h/2$ from the surface of the detector. In order to utilize an analytical expression given by Prata [5] for a case of coaxial, parallel circular source and detector, we approximate our square source with a circular source of a radius of the inscribed circle of the square. The averaged solid angle is estimated with the use of Eqs. (39), (40) and (41) given by Prata [5].

Fig. 2S The contact configuration between the cylindrical detector and a cylindrical homogeneous source of height h

Rd: Radius of cylindrical detector. Rs: Radius of inscribed circle of square source.

Note 3: Effect of self-attenuation

The concentration of ^{40}K is uniform in the source. Due to attenuation in the KCl cylinder, however, the detector on the top of the cylinder sees the concentration which decreases according to a familiar equation, $C(l) = C_0 \exp(-\mu\, l)$, where l is a distance from the top , C_0 is the concentration at the top of cylinder, and μ is the attenuation coefficient. Therefore, the actual number of photons which reach the top of the cylinder of height d is given by

$$C_0 \int_0^d \exp(-\mu\, l)\mathrm{d}\, l \; = C_0\, [1 - \exp(-\mu\, d)]\, /\mu,$$

while it is $C_0\, d$ for no absorption case.

Then, the effect of self-attenuation is expressed by a ratio, R_a, of the with-attenuation case to no-attenuation case,

$$R_a = [1 - \exp(-\mu\, d)]\, /(\mu\, d).$$

Although the density of solid KCl is 1.987 g/cm^3, that of our packed powder source is 1.26 g/cm^3. The mass energy attenuation coefficient of KCl is 5.03×10^{-2} cm^2/g at 1.5 MeV. Then, the attenuation coefficient for the test source μ becomes 6.34×10^{-2} cm^{-1}. We get $R_a = 0.911$.

----

1. 5 Uncertainty in estimation of count rate

The uncertainty involved in the above calculations is mainly in the detection efficiency and peak to total ratio which are read by the present authors from graphs published by Saint-Gobain Crystals [3], and in the estimation of the solid angle coverage. The overall uncertainty could be ±10%. Then, the estimated count rate becomes (17.1 ±1.7) cps. The estimated count rate is in good agreement with the observed count rate of 15.9 cps. The simple model calculation reproduces the observed count rate reasonably well.

Conclusion of Section 1

Under the contact configuration between the detector and the source, the observed count rate of 15.9 cps corresponds to an activity of ^{40}K of 5.81×10^3 Bq underneath the detector. The empirical conversion factor is 3.65×10^2 Bq/cps, that is, 1 cps corresponds to 3.65×10^2 Bq of ^{40}K underneath the detector. Statistical accuracy in determining the count rate is given by $1/\sqrt{N}$, where N is the number of accumulated counts under the photopeak of ^{40}K, 5.8×10^4. Therefore, the contribution of the statistical accuracy to the overall uncertainty in the empirically determined conversion factor is negligible.

4

2. Determination of the activity of ^{40}K in slabs of granite

We show that the activity of ^{40}K in slabs of granite is determined with the use of the obtained empirical conversion factor.

Two test slabs of granite, 121 mm×121 mm×t, t = 21.5 mm and 42.5 mm, are obtained from a quarry in northern part of the Abukuma mountains. The surface of the slab is wide enough to cover the window of the PTV for incoming gamma rays.

2. 1 Measurements of energy spectra

The measurements of the energy spectra are carried out in the same way as in the case of the KCl test source. A single Gaussian function is fitted to the photopeak at 1.46 MeV in each spectrum with the use of Origin Pro 2018 (Origin Lab Co., Northampton, MA, USA) to obtain the number of counts under the photopeak.

2. 2 Subtraction of background

Subtraction of the background spectrum is carried out in the similar way as in the case of the KCl test source. The density of granite, ρ, is 2.61 g/cm^3. According to Rahman et al. [6], the mass attenuation coefficient of granite at 1.5 MeV is 5.15×10^{-2} (cm^2/g). Then, at 1.5 MeV, μ = 0.1344 cm^{-1}.

2. 3 Concentration based on the measured count rate

An empirical way to estimate the activity of ^{40}K in the slabs is to use the conversion factor 3.65×10^2 Bq/cps which is obtained in Section 1. The results are summarized in Table 1S.

Table 1S Measured concentration of ^{40}K in the granite slabs

	Count rate (cps)	Net count rate (cps)	Activity of ^{40}K (Bq)	Mass of cylindrical portion of slab (kg)	Concentration of ^{40}K (Bq/kg)
Background	2.86				
21.5 mm slab	3.66	1.52	5.54×10^2	0.532	1.05×10^3
42.5 mm slab	4.07	2.45	8.94×10^2	1.050	0.85×10^3

The concentration is supposed to be the same in the two slabs. So, we take the mean of the above results, (1.0± 0.1) ×10^3 Bq/kg, as the value of concentration. According to the data published by National Institutes for Quantum and Radiological Science and Technology [7], the average concentration of ^{40}K in granite of Fukushima is 1.1×10^3 Bq/kg. The present results are in very good agreement with the published data. The

empirically determined conversion factor works well in the case of the contact configuration between the detector and the slabs of unknown concentration of ^{40}K.

2. 4 Estimated count rates based on the model calculation

Using the empirically determined concentration of ^{40}K in the slabs (1.0×10^3 Bq/kg), we see if our simple model calculations described in Section 1.4 reproduce the observed count rates for the slabs. The same assumptions are made, that is, the detector and the source are in the contact configuration, and the detector sees only the underneath cylindrical part of the slab. The factors 1, 2 and 3 are the same as those used for the KCl test source. The ratio of the solid angle to 4π and the effect of self-attenuation in the source are calculated for the two slabs. The results are summarized in Table 2S.

Table 2S Estimated count rates of the granite slabs

	Self-attenuation correction	Ratio of solid angle to 4π	Activity in cylindrical portion (Bq)	Estimated count rate (cps)
21.5 mm slab	0.868	0.405	0.532×10^3	1.7
42.5 mm slab	0.761	0.320	1.05×10^3	2.3

The count rate for 21.5 mm slab is 1.7 cps which is a little higher than the observed one, 1.52 cps. The count rate for 42.5 mm slab is 2.3 cps which is a little lower than that of observed one, 2.45 cps. However, in the both cases the uncertainty in the calculations is $\pm10\%$. Again, the simple model calculations work reasonably well.

Conclusion of Section 2

It is concluded that the concentration of ^{40}K in the granite rock of the Abukuma mountains is $(1.0 \pm 0.1) \times10^3$ Bq/kg which is in good agreement with the previously published data. The empirically determined conversion factor is reliable as long as the contact configuration between the detector and the source is established. In other words, the count rate of the photopeak of 1.46 MeV gamma rays from ^{40}K can be a good measure for establishment of the contact configuration.

3. Interpretation of the count rates of ^{40}K shown in Fig. 3 of Part 1

So far, we have examined the case that our detector contacts the surface of flat granitic rock and the detector receives gamma rays only from the underneath cylindrical part of the granitic rock where ^{40}K is uniformly distributed. As mentioned in Part 1, the areas

we have surveyed are under-water east foot of the Abukuma mountains which consist mostly of granitic rock. The mean count rate of the photopeak of ^{40}K shown in Fig. 3 in Part 1 is 2.79 cps (1674 counts/600 s).

In order to interpret the mean count rate of 2.79 cps we extend the measurements of the count rate of the 1.46 MeV photopeak to 61 mm thick granite slab and 81 mm thick one. The background subtraction is made in the same way as in Section 2.2. The results are 3.06 cps for 61 mm thick slab and 3.38 cps for 81 mm thick slab. These results together with the results of 21.5 mm thick and 42.5 mm thick slabs are true only for the case that the detector receives gamma rays only from the underneath cylindrical source diameter of which is close to that of the detector. There is no ^{40}K source outside the cylinder except the background from wall and floor. Actual situation at the bottom of reefs, however, is that the source is a heap of rock. Then, the detector receives gamma rays from all parts of the rock on which the detector lands, not just from the underneath cylindrical part. Therefore, the above-mentioned thickness dependence of the count rate can only be a guide to estimate the order of magnitude of the count rate in the actual situation. In this sense the observed count rate of 2.79 cps is quite reasonable. A remarkable feature in Fig. 3 of Part 1 is the uniformity of the count rates over the measured points. This fact strongly suggests that the contact configuration between the detector and a flat part of the surface of rock is established at every measured point.

The observed near uniformity of the count rates within ±6% shown in Part 1 can be interpreted as follows:
Extreme case 1: the concentration of ^{40}K could be different for each point as mentioned in Section 2.1 of Part 1, but the contact is established without appreciable uncertainty.
Extreme case 2: the concentration of ^{40}K is same for each point, but the contact is not always same for each point.
The surface of rock in the bottom of sea is expected to be not as flat and smooth as the surface of the slabs we used. Considering that we have no means to examine how flat the surface of rock is, it is plausible for us to adopt the Extreme case 2. Then, it can be safely said that the uncertainty in the contact is around ±6%. However, since the count rates at almost all points are in the width of ±10% of the mean, it is safer to say that the uncertainty in contact is ±10% at most. Then, the same can be said to the uncertainty in determination of the measured levels of ^{137}Cs.

Conclusion of Section 3
The values and their near uniformity in the measured count rate of the photopeak of ^{40}K firmly indicate that the contact configuration between the detector and a flat part of the

rock surface is established at the bottom of the sea. Therefore, our measurement of the level of ^{137}Cs on the surface of rock is credible with uncertainty of ± 10% at most.

References

1. Suzuki F, Ohashi H, Nogami K, Shibata H, Arakawa H, Umeda K, Kobayasi T, and Shiotani N (2024) On residual ^{137}Cs on shallow rugged reefs lying inshore of Fukushima: Part 1: Levels, distribution, and flux of radiations.

2. XCOM: Photon Cross Sections Data. https://physics.nist.gov/PhysRefData/Xcom/html/xcom1.html (Accessed Jan. 7, 2024)

3. Saint-Gobain Crystals (2020) Efficiency Calculations for Selected Scintillators. https://vepp2k.inp.nsk.su/~inest/halometer/SGC_Efficiency_Calculations.pdf (Accessed Jan. 7, 2024).

4. Legg J C and Seaman G G (1976) Nuclear and Atomic Spectroscopy, in: Williams, D. (Ed.), Methods of Experimental Physics Vol. 13-Part A. Spectroscopy. Academic Press, New York, pp115-147.

5. Prata M J (2004) Analytical calculation of the solid angle defined by a cylindrical detector and a point cosine source with parallel axes. Radiat. Phys. Chem. 69:273-279.

6. Rahman K N, Abdullah S A, and Gazzaz M A (1984) Studies on the radiation absorption characteristics of various rocks, Nuclear Engineering Department, King Abdulaziz University.

7. National Institutes for Quantum and Radiological Science and Technology https://www.nirs.qst.go.jp/db/anzendb/NORMDB/ENG/1_bussitunokensaku.php, In-depth data→ Rock and mineral→ Granite→Individual radioactive data. (Accessed Jan. 7, 2024).